

# Spatiotemporal Dynamics of Intratumoral Immune Cells Reveal the Immune Landscape in Human Cancer

Gabriela Bindea,<sup>1,2,3,11</sup> Bernhard Mlecnik,<sup>1,2,3,11</sup> Marie Tosolini,<sup>1,2,3</sup> Amos Kirilovsky,<sup>1,2,3</sup> Maximilian Waldner,<sup>1,2,3,4</sup> Anna C. Obenauf,<sup>5</sup> Helen Angell,<sup>1,2,3</sup> Tessa Fredriksen,<sup>1,2,3</sup> Lucie Lafontaine,<sup>1,2,3</sup> Anne Berger,<sup>6</sup> Patrick Bruneval,<sup>7</sup> Wolf Herman Fridman,<sup>2,3,9</sup> Christoph Becker,<sup>4</sup> Franck Pagès,<sup>1,2,3,8</sup> Michael R. Speicher,<sup>5</sup> Zlatko Trajanoski,<sup>10</sup> and Jérôme Galon<sup>1,2,3,6,\*</sup>

<sup>1</sup>INSERM U872, Laboratory of Integrative Cancer Immunology, Paris 75006, France

<sup>2</sup>Université Paris Descartes, Paris 75006, France

<sup>3</sup>Cordeliers Research Centre, Université Pierre et Marie Curie Paris 6, Paris 75006, France

<sup>4</sup>University of Erlangen-Nuremberg, Erlangen 91001, Germany

<sup>5</sup>Institute of Human Genetics, Medical University of Graz, Graz 8010, Austria

<sup>6</sup>Department of General and Digestive Surgery, Assistance Publique-Hopitaux de Paris, Paris 75015, France

<sup>7</sup>Department of Pathology, Georges Pompidou European Hospital, Paris 75015, France

<sup>8</sup>Department of Immunology, Georges Pompidou European Hospital, Paris 75015, France

<sup>9</sup>INSERM U872, Team 13, Paris 75006, France

<sup>10</sup>Biocenter, Section for Bioinformatics, Innsbruck Medical University, Innsbruck 6020, Austria

<sup>11</sup>These authors contributed equally to this work

\*Correspondence: [jerome.galon@crc.jussieu.fr](mailto:jerome.galon@crc.jussieu.fr)

<http://dx.doi.org/10.1016/j.immuni.2013.10.003>

## SUMMARY

The complex interactions between tumors and their microenvironment remain to be elucidated. Combining large-scale approaches, we examined the spatio-temporal dynamics of 28 different immune cell types (immunome) infiltrating tumors. We found that the immune infiltrate composition changed at each tumor stage and that particular cells had a major impact on survival. Densities of T follicular helper (Tfh) cells and innate cells increased, whereas most T cell densities decreased along with tumor progression. The number of B cells, which are key players in the core immune network and are associated with prolonged survival, increased at a late stage and showed a dual effect on recurrence and tumor progression. The immune control relevance was demonstrated in three endoscopic orthotopic colon-cancer mouse models. Genomic instability of the chemokine CXCL13 was a mechanism associated with Tfh and B cell infiltration. CXCL13 and IL21 were pivotal factors for the Tfh/B cell axis correlating with survival. This integrative study reveals the immune landscape in human colorectal cancer and the major hallmarks of the microenvironment associated with tumor progression and recurrence.

## INTRODUCTION

Cancer is a complex disease involving interactions between the tumor and the immune system (Finn, 2008). We have reported that a coordinated Th1 cell and cytotoxic immune infiltration both in the center and in the invasive margin of human colorectal

tumors is associated with a favorable clinical outcome in terms of local tumor spreading, disease-free survival, and overall survival. In contrast, a low density of T cells was associated with a poor prognosis (Galon et al., 2006; Galon et al., 2007; Pagès et al., 2005). In fact, the various clinical and histopathologic criteria currently available (Jemal et al., 2006; Weitz et al., 2005) show that the T cell immune infiltrate is the most important predictive criterion for patient survival (Atreya and Neurath, 2008; Bindea et al., 2010; Galon et al., 2006; Mlecnik et al., 2011; Pagès et al., 2009). This association is also supported by mouse models of immunosurveillance and immunoediting (Koebel et al., 2007; Schreiber et al., 2011; Shankaran et al., 2001; Smyth et al., 2006). Advances in cellular immunology and tumor biology are facilitating new approaches toward adoptive T cell therapy (June, 2007b) and leading to promising results (June, 2007a). Analysis of colorectal and other tumors have confirmed the positive impact of T cells (reviewed in (Fridman et al., 2012)). However, cells infiltrating tumors are highly heterogeneous, and most of the components of myeloid and lymphoid compartments are represented. Analysis of how immune cells other than Th1 and cytotoxic lymphocytes affect clinical outcome has often yielded contradictory results. In addition, no comprehensive analysis of the local coordination of the various immune compartments, nor of the genome plasticity of cancer cells, has been conducted in the same patients.

To gain deeper insights into tumor progression and tumor recurrence mechanisms in human colorectal cancer (CRC), we performed integrative analyses. Our systems approach to cancer is grounded in the idea that the host-immune response and tumor progression reflect perturbations at the gene and protein level and that regulatory networks differ over time and with clinical outcome (Mlecnik et al., 2010b; Wang et al., 2004; Wang et al., 2008).

To understand the complex spatiotemporal dynamics of the tumor-immune interaction during tumor progression, we used several experimental approaches and visualization methods. We investigated most of the tumor-immune infiltrates as well

as sources of genetic diversity that could influence the generation of immune responses. We built a compendium of mRNA transcripts specific for most innate and adaptive immune cell subpopulations that constituted the “immunome.” We analyzed the immunome of 105 patients with colorectal carcinoma. We also used quantitative real-time PCR (qPCR) and tissue microarrays (TMAs) to evaluate the immune reaction within the center (CT) and at the invasive margin (IM) of the tumor and to examine its changes as a function of the tumor stage. The impact on patient survival of all immune cells infiltrating tumors was shown. Chromosomal instability of all chemokines and chemokine receptors was evaluated, and mechanisms associated with major immune cell infiltration were revealed through the use of human samples, *in vitro* assays, and several mouse models of CRC. Here, we present the immunome analysis as what we refer to as the “immune landscape,” a hallmark of the tumor microenvironment associated with tumor progression and recurrence in CRC patients.

## RESULTS

### Analysis of Immune Cell Subpopulations Defining the Immunome

We characterized the immune reaction in the tumor microenvironment by establishing a reference, the immunome compendium. In order to build this compendium, we used publicly available data from purified immune cell subsets (Chtanova et al., 2005; Hycza et al., 2007; Wendt et al., 2006) to compare the transcriptional profile of most immune cell subpopulations. We investigated both innate immune cells (dendritic cells [DCs], immature DCs [iDCs], activated DCs [aDCs], eosinophils, mast cells, macrophages, natural killer cells [NKs], NK CD56<sup>dim</sup> cells, NK CD56<sup>bright</sup> cells, and neutrophils) and adaptive immune cells (B, T helper 1 [Th1], Th2, T gamma delta [T $\gamma\delta$ ], CD8<sup>+</sup> T, T central memory [Tcm], T effector memory [Tem], and T follicular helper [Tfh] cells). Additionally, data from normal mucosa (Ancona et al., 2006) and colon cancer cell lines (Provenzani et al., 2006) were integrated with the immune data in a comprehensive collection of microarray data sets. Highly distinctive transcriptional profiles of all cell types were selected (Figure 1A; see also Table S1 in the Supplemental Information available with this article online). The selection was completed with known markers of subpopulations of T helper 17 (Th17) cells, regulatory T (Treg) cells, and blood and lymphatic vessels present in the tumor microenvironment but not included in this collection. A total of 577 genes (681 Affymetrix probes) constituted the normal reference that was further used for investigation of the immune reaction in CRC patients.

We then performed microarray expression experiments and analyzed the 681 probes in tumors from 105 CRC patients and five histologically normal colon mucosa. Two clusters of patients were found, and 372 probes were significantly differentially expressed between the two groups (Figure 1B). As shown in Figure S1A and Table S2, the patterns of expression that characterized the group of patients with significantly prolonged disease-free survival (cluster 1) were different than those that characterized patients with an unfavorable outcome (cluster 2) (hazard ratio [HR] = 2.0 (95% CI, 1.1–3.7;  $p = 0.02$ ). An overrepresentation of highly expressed genes specific for T cell popu-

lations and subpopulations of Th1, T $\gamma\delta$ , cytotoxic T cells as well as for macrophages and mast cells was significantly associated with the patient cluster 1 (all  $p$  values < 0.05). In comparison, patient cluster 2 showed an overrepresentation of highly expressed genes specific for eosinophil, Tcm, Th2, Th17, Treg, and NK cell subpopulations (all  $p$  values < 0.05). As compared to the cancer cell line markers that associated to cluster 2, lymph vessel and normal mucosa makers were significantly overrepresented in cluster 1 (all  $p$  values < 0.05). Functional analysis of the immune signature was performed with CluePedia and ClueGO (Bindea et al., 2013; Bindea et al., 2009; Figure S1B). The genes highly expressed in cluster 1 were mainly associated with cytotoxic T cell surface molecules, T helper cell surface molecules, and chemokine-related terms, and functions related to endothelial cell migration. In contrast, cluster 2 patients showed a different immune pattern, involving genes with roles in IL-2 signaling and in the regulation of adaptive immune responses. Thus, patients have diverse intra-tumor immunome patterns that correlate with different clinical outcomes.

### Coordination of Immunome Gene Expression

We used a more sensitive method, qPCR, to investigate the expression of 81 representative genes (selected from the 577 genes in Figure 1) in 153 CRC patients (Figure 2 and Table S3). Most of the 81 selected genes were known immune membrane receptors. When we compared the expression of these 81 markers on immunome-positive cell types versus all other negative cells, the median increase was 92-fold (95% confidence interval [CI]: 4.5–490), showing the strong overexpression of these genes in a specific cell type. Herein, multiple techniques and experimental approaches (including DNA microarray [Affymetrix], quantitative PCR [qPCR], fluorescence-activated cell sorting [FACS], immunohistochemistry, and mouse models) were used, and strong correlations were found with different approaches (Figure S2). Markers specific for the same cell type strongly correlated and clustered together (Figure 2 and Figure S3). A positive correlation between markers of different cell types was found as well, and functional associations of comodulated genes were defined (Figure 2 and Table S4). Unsupervised clustering revealed three main functional associations (clusters 1, 2, and 3) at the tumor microenvironment. SW480 cancer cells, neutrophils, and Th17 cell markers grouped in cluster 1 and did not correlate with other cell-type markers. Two other clusters showed adaptive (cluster 2) and innate (cluster 3) immune cell marker predominance. Within the innate cluster, overrepresentations of markers of mast cells and eosinophils (cluster 4), dendritic cells (cluster 5), and macrophages (cluster 6) were found. The adaptive immune cluster (T, B, and Tfh cells) functionally grouped into different subclusters (clusters 7, 8, and 9). Particular innate and adaptive markers were correlated with one another. NK cell markers clustered with CD8<sup>+</sup> T cell markers, reflecting the common cytotoxic properties of these cells (cluster 7). Within the adaptive cluster, besides a coordination of T cell subpopulation markers, B cells and Tfh cell markers (cluster 8) presented a strong and significant ( $p < 0.0001$ ) correlation with the T cell markers (Table S4). Th1 and overall T cell markers formed cluster 9. Thus, a coherent profile emerged from the unsupervised clustering of the gene-gene correlation matrix. Major

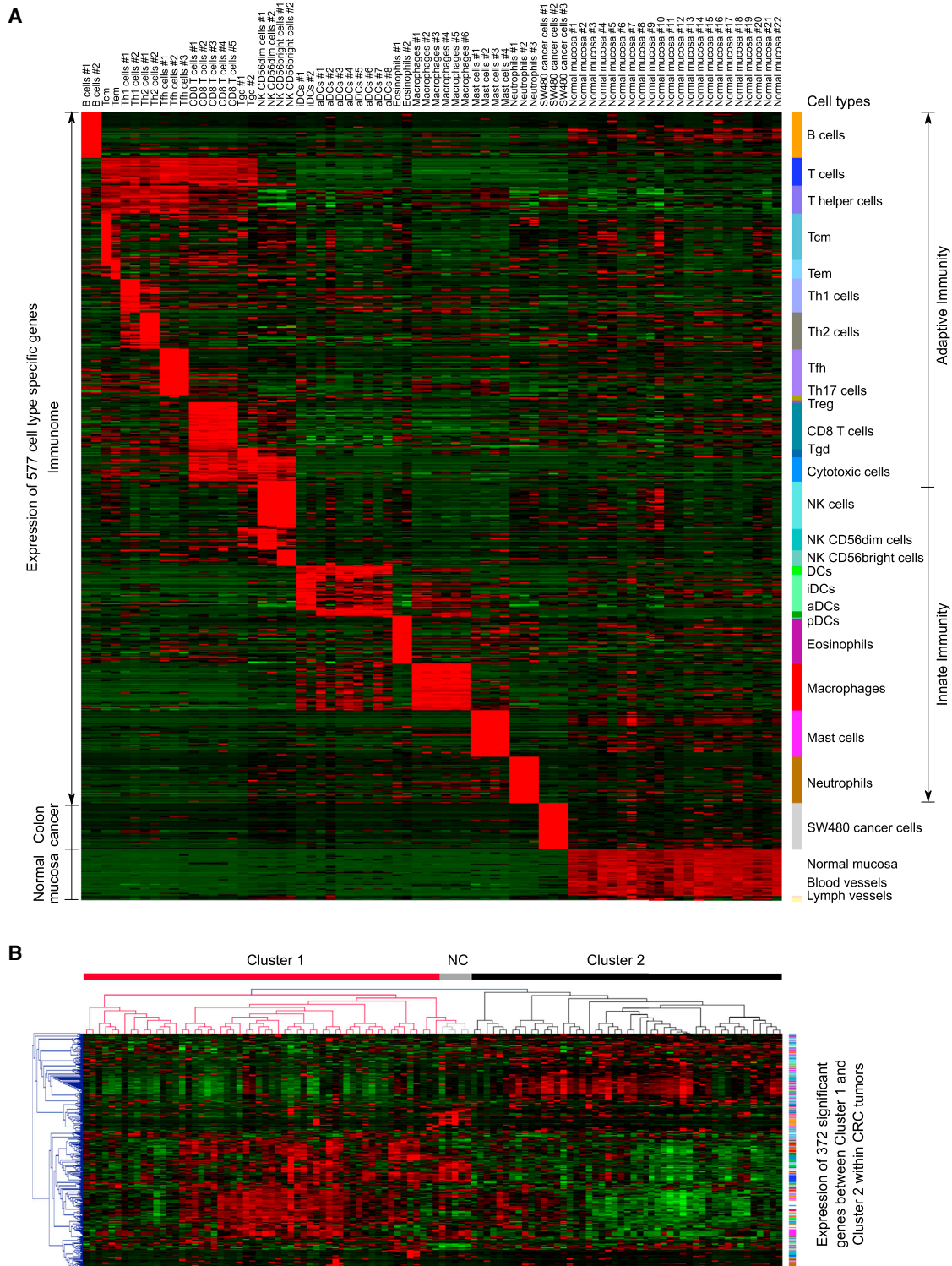


**Figure 1. Immunome Gene Selection**

(A) Transcriptome data for purified adaptive and innate immune cells (immunome), a colon cancer cell line, normal mucosa, blood, and lymph vessels were normalized with Genesis (Sturm et al., 2002). Five hundred seventy-seven cell-type-specific genes (681 Affymetrix probes) are shown. Highly expressed genes are in red, and lowly expressed genes are in green. The 28 cell types are shown in a colored bar (right). This collection comprises, besides genes specific for particular subpopulations, genes highly expressed by immune cell populations (DCs, T cells, T helper cells, and NK cells) and by cells with common cytotoxic properties (cytotoxic cells: CD8 T cells, T $\gamma$  $\delta$ , and NK cells).

(legend continued on next page)

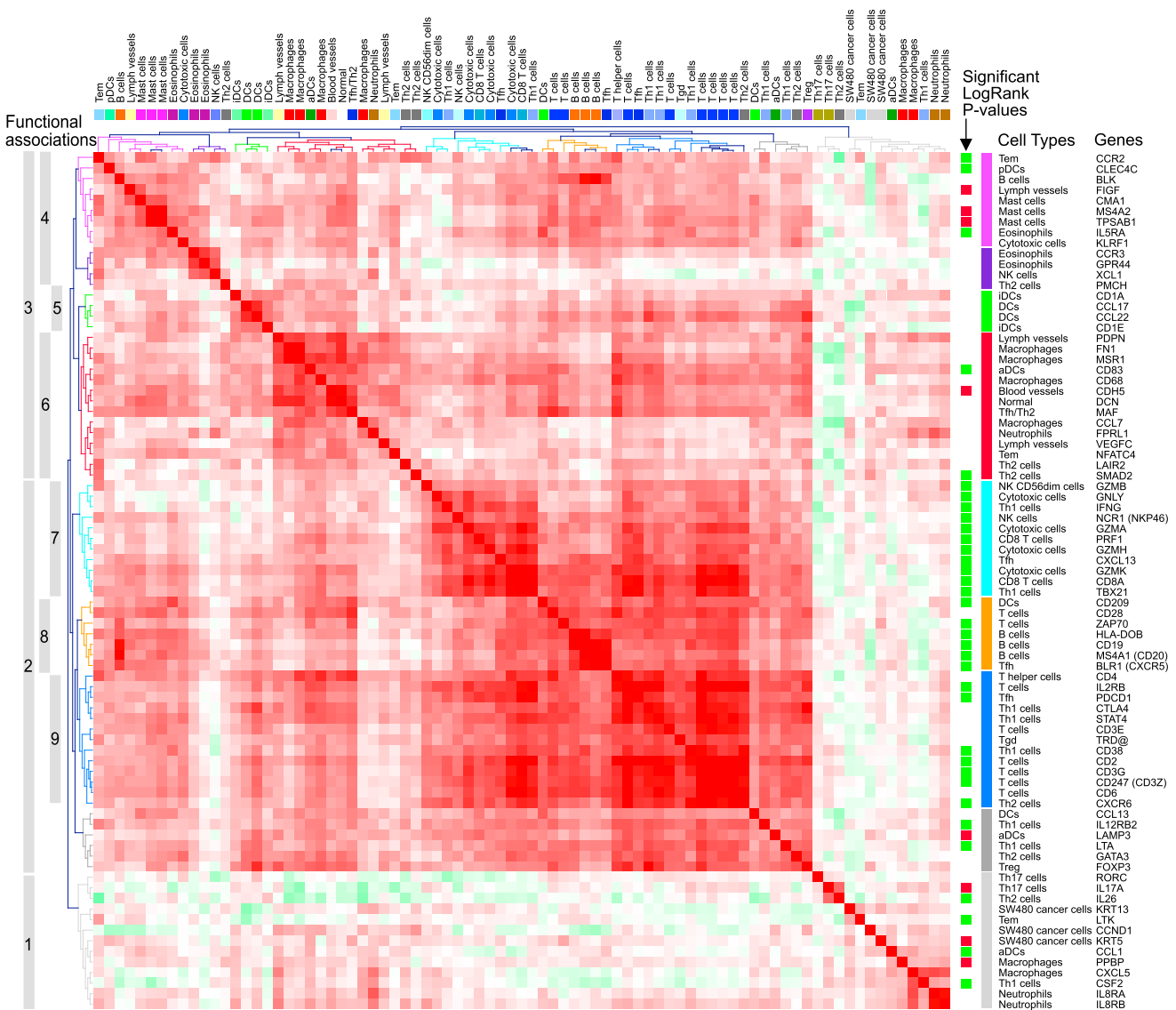


**Figure 2. Gene-Gene Correlation Matrix Characterizing the Tumor Microenvironment**

Pearson-correlation matrix of 81 cell-type-specific genes tested by qPCR on 153 colorectal CRC patients. The correlation matrix was subjected to unsupervised hierarchical clustering (Euclidean distance measurement, average linkage clustering). Each colored square within the figure illustrates the correlation between two genes for all the patients. Red color illustrates a very strong positive correlation ( $r = 0.9$ ,  $p < 0.00001$ ), white no correlation ( $r = 0$ ), and green a negative correlation ( $r = -0.9$ ). The distribution of cell types corresponding to the clustered genes is shown in a colored bar (top). Functional clusters of comodulated markers are shown (left). For each cluster, the cell type overrepresentation was evaluated with a Fisher's exact test (Table S4). Tumor recurrence analyses are presented (right). Genes for which impact on disease-free survival was found to be significant by a log-rank test and that had HR < 1 (good impact on patient outcome) are marked with a green square, and those with HR > 1 (bad outcome) are marked with a red square. See also Figures S2 and S3 and Tables S3 and S4.

clusters (7, 8, and 9) revealed an intricate coordination of immune cell subpopulation markers within the tumor.

Knowing the strong impact of the T cell markers on patient survival, we further investigated cells having a similar functional profile in tumors. We performed additional quantitative qPCR experiments to investigate how B cell markers might be associ-

ated with patient survival. In the two groups of patients defined in Figure 1B, with good (cluster 1) and bad (cluster 2) outcomes, we analyzed major histocompatibility complex (MHC)-II-related genes and B cell costimulation-related genes, as well as genes related to T cells, Tfh cells, MHC-I, and inflammation. Patients with prolonged survival had a significant increase in the

(B) Six hundred eighty-one probes were investigated in 105 CRC tumors and five distant normal colon (NC) samples. The data were normalized and hierarchically clustered (Pearson uncentered algorithm, average linkage). Two patient clusters were revealed. Three hundred seventy-two probes for which a t test showed a significant difference ( $p$  value < 0.05) between patient clusters 1 and 2 are shown. Highly expressed genes are shown in red, and lowly expressed genes are in green. See also Figure S1 and Tables S1 and S2.

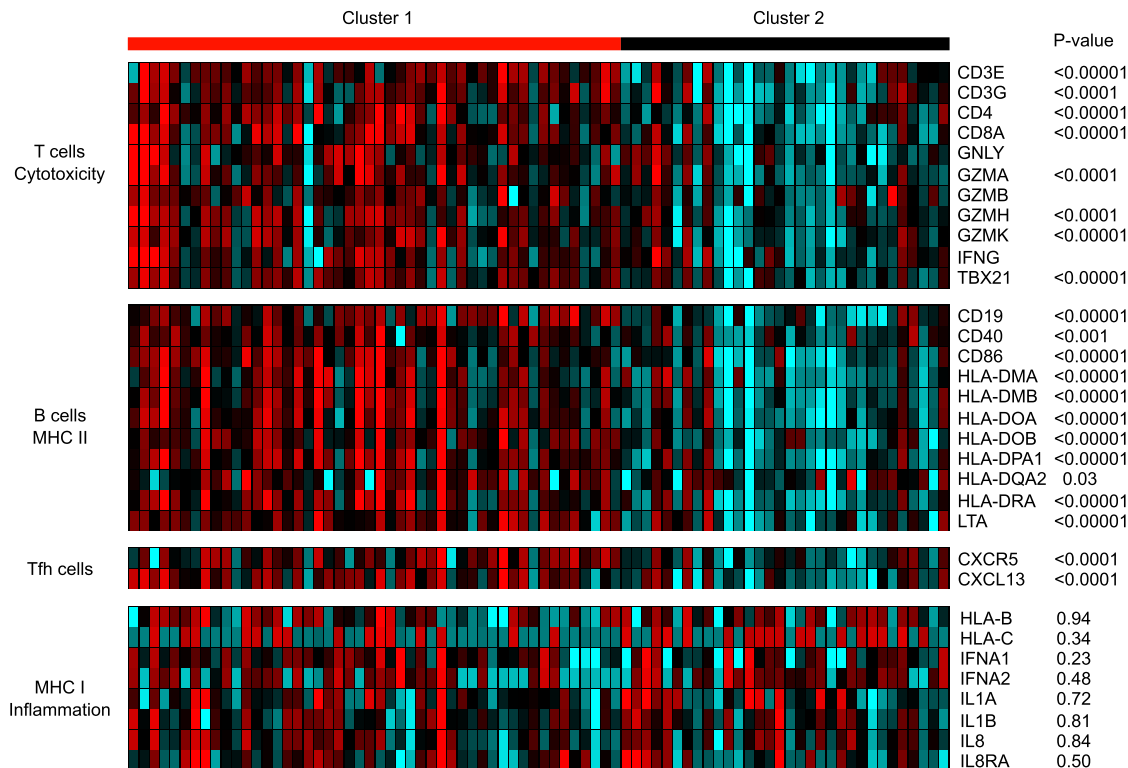


**Figure 3. Expression of MHC-, Costimulation-, and Inflammatory-Related Genes in CRC Patients from Clusters 1 and 2**

Gene expression levels were assessed by qPCR and determined with Ct values (threshold cycle) normalized to 18S (dCT). Heat-map representation of the gene clusters for different immune functions are shown. Genes are plotted from the minimal level of expression (blue) to the maximal level (red). The Mann-Whitney test was used for comparison of the expression levels of each gene between patient groups.

expression of genes related to MHC-II, B cell costimulation, T cells, and Tfh cells. In contrast, no significant difference was found in the expression of MHC-I- and inflammation-related genes (Figure 3).

The tight coordination of adaptive immune markers found at the tumor microenvironment could be a fundamental feature of the host defense in response to tumor development.

#### Analysis of Immune Subpopulations In Situ

The expression of markers for Tfh cells, a cell type known to “help” the generation of B-cell-mediated immune responses (King et al., 2008), showed a strong correlation with the B cell markers. Using tissue microarrays, we next examined the different immune cell subpopulations in the CT and at the IM of 107 CRC patients (Figure 4A; see also Figure S4). All the immune cell subsets tested were found within the tumor at varying cell densities. Furthermore, the composition of the immune infiltrate was different in the CT versus the IM region. It was of interest to note the predominance of the B cells at the IM compared to the CT. Greater numbers of the T cell subsets (CD3, CD45RO, CD8, CD57, and CXCR5) were also present at the IM. Using four-color fluorescent immunohistochemistry, we confirmed the presence of T cells, Tfh cells, and B cells in situ within CRC tumors (Figure 4B). Importantly, the immune reaction appeared to evolve with tumor progression from stages T1 to T4 (Figure 4C). Most of the T cell subpopulation markers, CD3, CD8, CD57, CD45RO, and FOXP3 (with the exception of those for Tfh cells),

were highly expressed at early stage (T1) and then decreased with tumor progression. In contrast, the density of B cells increased with tumor stage, as did that of the innate immune cells such as neutrophils, mast cells, iDCs, pDCs, and macrophages.

We have visualized, in a format that we refer to as “flower plot,” the n-fold change of the density of each of the immune cell markers as a function of the tumor stage at both the CT and the IM (Figure S4). Each transition stage was associated with a new immune profile at the tumor site. Immune subpopulations varied in density profiles at the CT and IM with time and tumor progression. The transition of tumor stages T1–T4 was characterized by the increase or decrease of immune cell densities. The evolution and spatial distribution of these subpopulations in tumor regions might affect tumor recurrence.

#### Importance of the Intratumoral Immune Landscape

We next studied the contribution of the immune landscape to tumor recurrence and showed that distinct immune profiles are associated with significantly different prognoses (relapse risks) (Figure 5). Most of the T cell markers, including CD8<sup>+</sup> for T, Th1, and Tem cells, were logrank significant and associated with a good prognosis (disease-free survival, DFS; HR < 1), confirming our previous reports (Galon et al., 2006). We found that a high expression of Tfh and B cell genes was also strongly associated with a good prognosis (Table S4 and

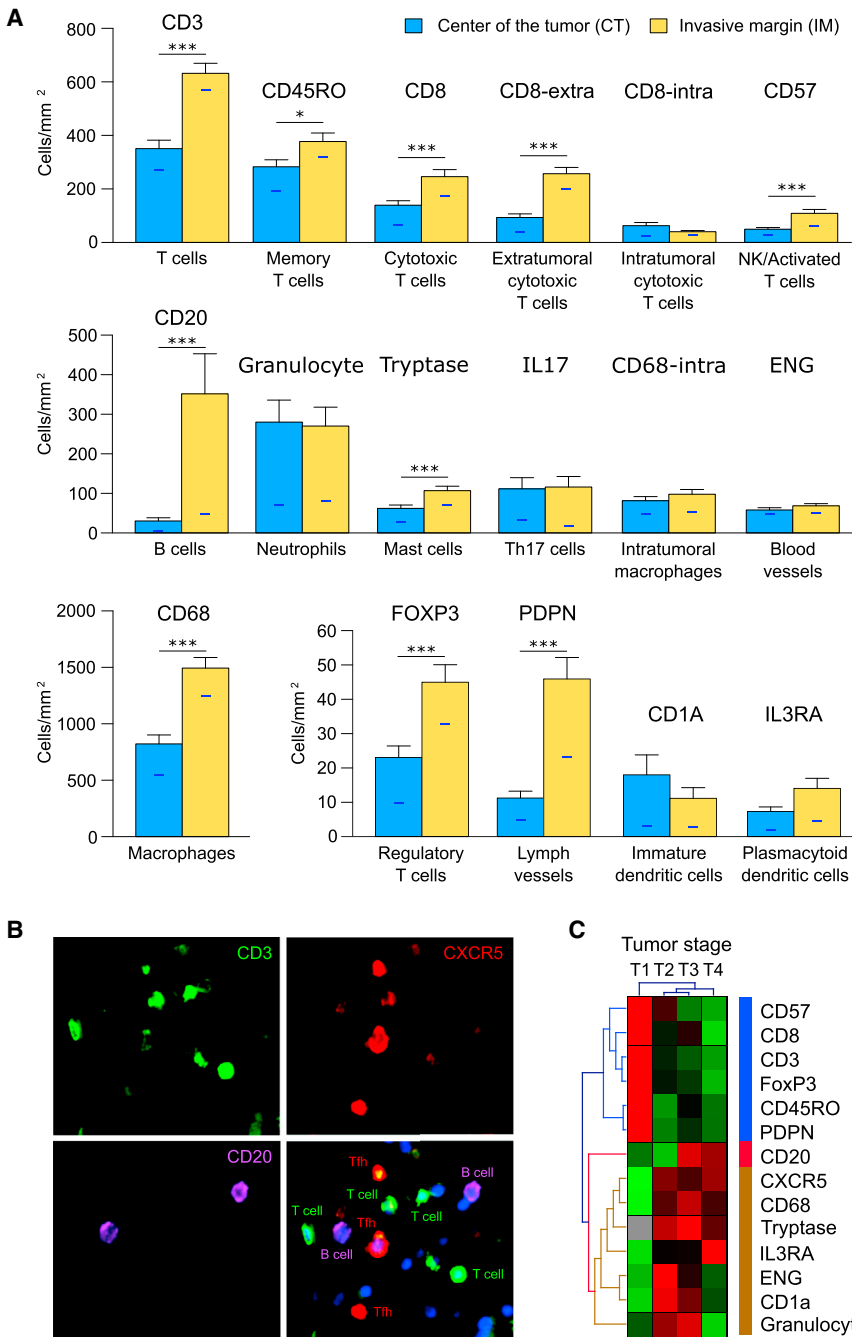


**Figure 4. Analysis of Intratumoral Immune Cell Densities Relative to the Tumor Stage**

(A) Immune cell infiltrates from 107 CRC patients were analyzed by tissue microarray (TMA). T cells (quantified with marker CD3), cytotoxic T cells (CD8), memory T cells (CD45RO), Treg cells (FOXP3), activated T or NK cells (CD57), Tfh cells (CXCR5), Th17 cells (IL-17), B cells (CD20), iDCs (CD1a), pDCs (IL3RA), macrophages (CD68), mast cells (Tryptase), neutrophils (granulocyte), blood vessels (ENG), and lymph vessels (PDPN) were quantified by immunohistochemistry. For cells marked by CD8 and CD68, the cell density was evaluated as total cell density of extratumoral cells (within the stroma) and intratumoral cells (within the tumor glands). The density of the cells was recorded as the number of positive cells per mm<sup>2</sup> surface area by use of a dedicated image-analysis workstation (Spot Browser ALPHELYS). The mean (± SEM) cell densities in the CT (light blue bars) and IM (orange bars) were compared. The tested marker for each cell type is shown in the top of the bars. In dark blue, the median cell count/mm<sup>2</sup> is shown. The test that was suggested on the basis of the Shapiro test result was the Wilcoxon-Mann-Whitney test for all the cell types. \*\*\*p < 0.001, \*\*0.001 ≤ p < 0.05, and \*0.05 ≤ p < 0.1.

(B) Immune cell populations present at the tumor site were visualized by four-color immunohistochemistry. Tumors were stained for CD3-positive T cells (green), CD20-positive B cells (pink), CXCR5-positive Tfh cells (red), and the nucleus (DAPI, blue). Tfh cells (double stained for CD3 and CXCR5) are present at the tumor site in close proximity to B cells and other T cells.

(C) The evolution in time of the mean cell density (TMA data) in 107 CRC patients. The data were normalized and hierarchically clustered (Manhattan distance, single linkage). Highly expressed genes are shown in red, and lowly expressed genes are shown in green. The T cell markers (CD57, CD3, CD8, FoxP3, and CD45RO) and lymph-node marker (PDPN) are clustered together (blue cluster). Their expression decreased with tumor stage from T1 to T4. In contrast, the mean expression of CD20-positive B cells (represented in red) increased with progression to stage T4. A similar pattern can be seen for the innate cell markers (CD68, Tryptase, IL3RA, and granulocyte), CXCR5 (Tfh cells), and ENG, the blood vessel marker (brown cluster). See also Figure S4 and Table S4.

Figure S5). Furthermore, among innate immune cells, markers of NK cells, pDCs, aDCs, and eosinophils also exerted a moderate positive effect. In contrast to all other T cell subpopulations, Th17 cells negatively influenced the patient outcome (DFS, HR > 1, p < 0.05).

Correlation and survival analyses of the 81 qPCR genes were integrated in a Cytoscape (Shannon et al., 2003) network. Besides gene-gene interactions, complex interrelations between different immune cell types were revealed (Figure S3). A strong positive correlation between adaptive immune cell markers was present (Table S5) and had a positive impact on

the patient outcome. Although associated with the adaptive network, macrophages had no prognostic effect. The other immune cell populations had weaker correlations with the adaptive immune cell cluster and between themselves. All these results were confirmed at the protein level via in situ immunohistochemistry (Figure 5).

Based on the TMA data, a 3D visualization of the immune landscape in CRC allowed us to investigate the immune cell density patterns over time in situ and their impact on the patients' disease-free survival (Figure 5 and Movie S1). The network topology showed a clear separation between the two



tumor regions, each having a distinct and characteristic immune cell density pattern, as shown by the distribution of blue (CT) and yellow (IM) peaks. In each tumor region, a sub-network of T cell subpopulations (CD3 cells, CD8 cells, memory T cells, Treg cells, and activated T cells) could be found (Figure 5A). This analysis also revealed several unexpected observations. Within the tumor center, it was interesting to note the close correlation between B cells (CD20) and the T cell subset network (even though the actual number of B cells was small). There was an increased fraction of intratumoral CD8<sup>+</sup> T cells among cytotoxic T cells in the CT compared to the IM (34% versus 16%). At the tumor margin the density of B cells was elevated and correlated with the IM T cell network and, in particular, with memory T cells (indicated by marker CD45RO). Tfh cells (indicated by marker CXCR5) were infiltrating the tumor center were closely correlated with T cell subsets measured in the tumor margin. Furthermore, the macrophages were the only innate cells associated with the T cell network in both tumor regions, whereas the density of lymphatic vessels (quantified with marker podoplanin [PDPN]) correlated with the CT part of the T cell network. In contrast, other cell types, such as granulocytes, mast cells, and Th17 cells, were not associated with the core T cell network and showed no difference in their density between the CT and the IM. The density of iDCs and pDCs in the CT was not correlated with the density measured in IM. The local coordination shown in the T cell network underlines the existence of tumor-microenvironment compartments with different compositions that might influence the mobility and activity of T and B cells along with tumor progression. The evolution of the individual cell-type density during tumor progression (from T1 to T4 stages) can be visualized in a 3D animation (Movie S1).

We showed the impact of individual cell types on the DFS as reflected by peaks representing the HR (Figure 5B). It is evident that virtually all of the T cells in the network (except for Th17 and Tfh cells in the IM) exert a marked positive effect on the clinical outcome. A high density of B cells correlated with prolonged survival (CD20<sub>CT</sub> CD20<sub>IM</sub> HiHi versus LoLo, HR = 3.7 [95% CI: 1.9–7.6],  $p < 0.002$ ). The good prognostic impact of B cells was further validated in an independent cohort of 415 patients, (HR = 2.2 (95% CI: 1.4–3.6),  $p < 0.05$ ). Furthermore, a significant beneficial effect of IM B cells on DFS was observed when the IM B cell densities were combined with T cells densities (Table S6). In this regard, it was of interest that the Tfh cells (as shown by the density of CXCR5<sup>+</sup> cells in the CT) also exerted a positive effect. From the innate immune cells, only neutrophils and mast cells at the IM showed a moderate positive impact on patient survival, whereas macrophages and iDCs were slightly (almost but not quite significantly) associated with a bad outcome. The presence of lymphatic vessels was beneficial for patient survival. The strong correlation of B cells and Tfh cells, components of cells of adaptive immunity, as shown with both qPCR and TMA analyses underlines the importance of those cells in strengthening the protection against tumor recurrence (Deola et al., 2008). These adaptive immune cells are likely to ensure long-term survival of the patients because they can acquire a memory phenotype.

### Mechanisms Associated with CXCL13 Expression and Intratumoral Densities of Lymphocytes

Given the impact of the local immune reaction on a patient's survival, it was of major importance to understand mechanisms resulting in high or low densities of specific immune cells within the tumor. Genomic instability that generates genetic diversity could influence the generation of immune responses. We thus investigated the accumulation of amplifications or the presence of deletions of the chromosomal regions where all ( $n = 53$ ) chemokines and chemokine receptors are located. The chromosomal instability (CIN) in CRC tumors was analyzed by array comparative genomic hybridization (aCGH). As expected, we identified many gains and losses of chromosomal regions, as has been previously reported in colorectal cancer; for example, a gain of 8q and a loss of 8p has been reported (Tsafrir et al., 2006). An overview of the chromosomal location of the chemokines and their corresponding frequency of gains and losses in 109 CRC patients is shown (Figure 6A). The most frequently (>15%) amplified chemokines were located in chromosomes 7, 16, and 19. Frequently deleted cytokines (>15%) were located in chromosome 4 and 17.

The genomic alterations occurring in tumor cells could provoke changes in local chemokine expression. To evaluate this hypothesis, we compared the expression of the chemokines in patients with or without genomic alterations. We found nine chemokines with significantly different expression in patients with aberrations than in those without (Figure 6B). Two chemokines (CCL24 and CXCL9) showed significantly higher expression in patients who had a gain, whereas significantly lower expression was observed for seven deleted chemokines (CCL1, CCL26, CCR6, CXCL2, CXCL12, CXCL13, CXCL16) (Figure 6B). Using immunohistochemistry, we showed that tumor cells expressed CXCL13 (Figure 6C). We further illustrated that patients with CXCL13 deletion had decreased CXCL13 expression levels (Figure 6D). We stratified patients into three groups based on their genomic alterations (gain, loss, no aberration). Strikingly, survival analysis in patients with aberrations (HR = 2.44 [95% CI: 1.2–4.9],  $p < 0.05$ ) versus patients without genomic alterations revealed only two chemokines (CXCL2 and CXCL13) that conferred a significantly different risk to relapse when they were deleted (Figure 6B). Thus, patients with CXCL13 deletion have a significantly higher risk of relapse than do patients without aberrations, as illustrated by Kaplan-Meier curves (Figure 6E). We hypothesized that CXCL13 deletion within colorectal tumors could be a mechanism resulting in low densities of B cells and Tfh cells. We investigated the in situ densities of B cells and Tfh cells within different tumor regions from colorectal tumors (Figure 6F). Patients with CXCL13 deletion showed a lower density of B cells and Tfh cells in the IM region. To demonstrate the impact of CXCL13 produced by tumor cells, we isolated fresh tumor cells from colorectal tumors and cultured them for 24 hr. We used supernatants from tumor cells to induce the in vitro migration of immune infiltrating cells from the same tumors. CD4<sup>+</sup> T cells migrated when subjected to tumor cell supernatants, whereas NK cells and macrophages did not. Finally, anti-CXCL13 antibodies inhibited this migration, demonstrating the chemoattractant role of CXCL13 within tumors (Figure 6G). To validate the importance of Tfh-cell-related major soluble factors, we investigated the expression of CXCL13, IL21,

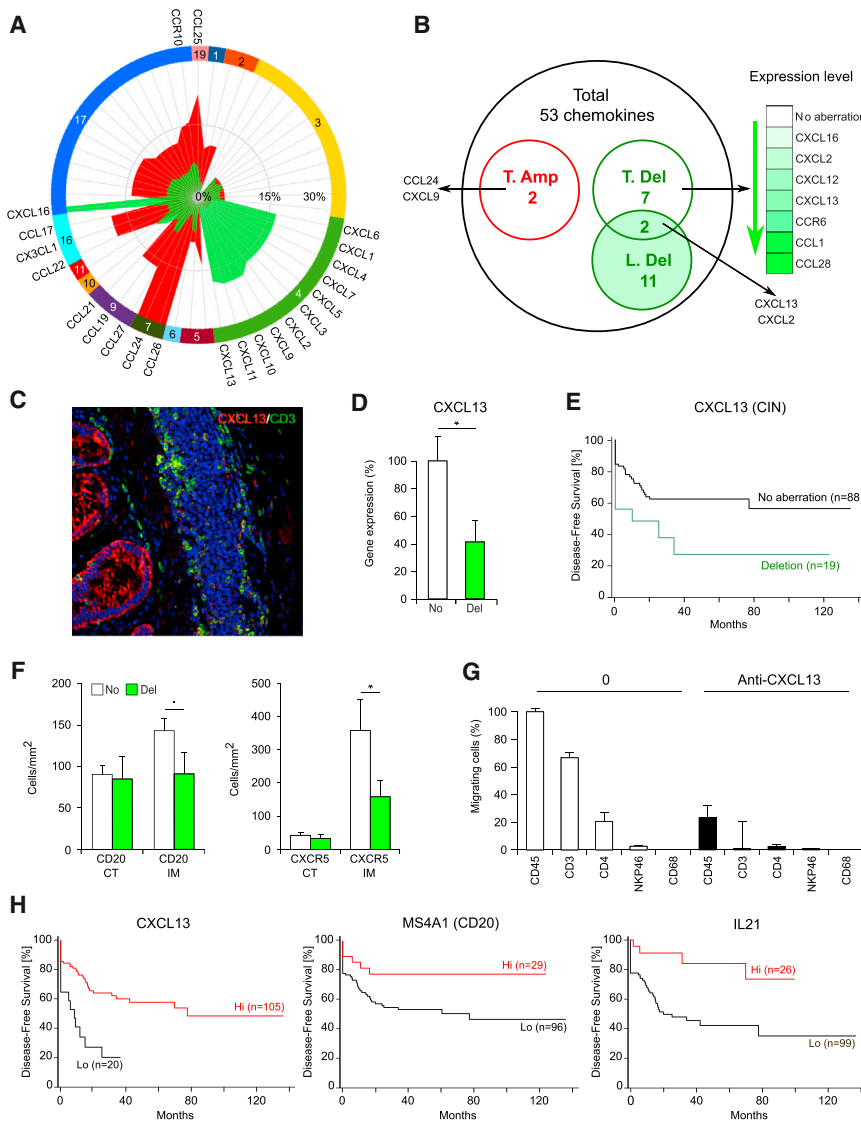


**Figure 6. Genomic Alterations in CRC Patients**

(A) The chromosomal location and the frequency of genomic alterations of 53 chemokines and chemokine receptors within colorectal tumors. Genomic alterations were investigated in 105 patients by aCGH. The shown frequency scale ranges from 0%–30%. The frequency of gains and losses is represented in red and green, respectively. The chemokine genes with alterations in more than 15% of the patients are underlined.

(B) Venn diagram showing the number of t-test and log-rank-test significant genes among the 53 chemokines. t-test significant cytokines with a gain (n = 2, red) or loss (n = 7, green) are shown. The expression level in aberration-containing patients compared to patients without aberrations is shown on the right side. Among all chemokines, 11 were log-rank-test significant, and among these, only 2 (CXCL2 and CXCL13) were also t-test significant with regard to their expression.

(C) CRC sections were assessed immunohistochemically with triple fluorescent stainings with DAPI (blue), a mouse anti-human CD3 antibody (green), and a mouse anti-human CXCL13 antibody (red).

(D) Histograms representing the mean ± SEM CXCL13 expression relative to that in patients without aberrations is shown. No aberration (No, white) and deletion (Del, green) patient groups are represented.

(E) Kaplan-Meier (KM) curves for DFS for patients with a chromosomal deletion (green) of CXCL13 versus patients without genetic alterations (black).

(F) Histograms represent the mean densities ± SEM of CD20+ and CXCR5+ cells as the number of positive cells/mm<sup>2</sup> of tissue at the IM (CD20-IM and CXCR5-IM) CT (CD20-CT and CXCR5-CT) of tumors from CRC patients. The mean density is represented for patients with a chromosomal deletion of CXCL13 (green columns) versus patients without genetic alterations (white columns).

(G) Tumor cells and tumor-infiltrating lymphocytes (TILs) were isolated. TILs were seeded in transwell chamber containing patient-matched tumor cell

supernatants with or without anti-CXCL13 neutralizing antibody. Migrating cells (indicated by markers CD45, CD3, CD4, NKP46, and CD68) were analyzed by flow cytometry after 24 hr. Data are presented as means ± SEM.

(H) Kaplan Meier curves for DFS for CXCL13 (the B cell chemoattractant), MS4A1 (CD20, a B-cell-specific gene), and IL21 showed significant separation between the group of highly expressed genes (Hi, red) versus the lowly expressed genes (Lo, black) at the minimum p-value cutoff.

Significantly different expression as well as log-rank significance are marked by an asterisk. See also Figure S6 and Table S6.

and B-cell-related markers (MS4A1 and CD19) in relation with DFS. High expression of B cell markers (CD19<sup>Hi</sup> versus CD19<sup>Lo</sup> [HR = 1.95 (95% CI: 1.1–3.5)] and MS4A1 [HR = 2.76 (95% CI: 1.0–7.6)], *p* < 0.05) and of Tfh cell markers (CXCL13 [HR = 3.2 (95% CI: 1.7–6.0)] and CXCR5 [HR = 1.96 (95% CI: 1.1–3.5)], *p* < 0.05) correlated with a significantly prolonged disease-free survival time (Figure 6H and Table S6). We further analyzed the mechanistic aspects of our findings. We correlated CXCL13 and IL21 expression with markers specific for immune cell subpopulations. A strong intratumor association of these factors with B, Tfh, Th1, and cytotoxic T cells was revealed. In contrast, they were not correlated with other cell populations (Figure S6). Thus, these results underline a mechanism by which CXCL13

could affect the intratumor densities of major immune cell subpopulations associated with the survival of the patients.

### Loss of the Adaptive Antitumor Immune Response Is Associated with Tumor Progression in Murine Orthotopic CRC Models

In order to further analyze the role the adaptive anti-tumor immune response, we developed a unique endoscopic orthotopic CRC model in mice. Mouse CRC cell line MC38 was injected endoscopically into the colonic submucosa of syngenic C57Bl/6 mice (Figure 7A). Tumor growth was monitored weekly via endoscopy. Within a few weeks, tumor cells built a continuously growing tumor mass in the intestinal wall. The morphology

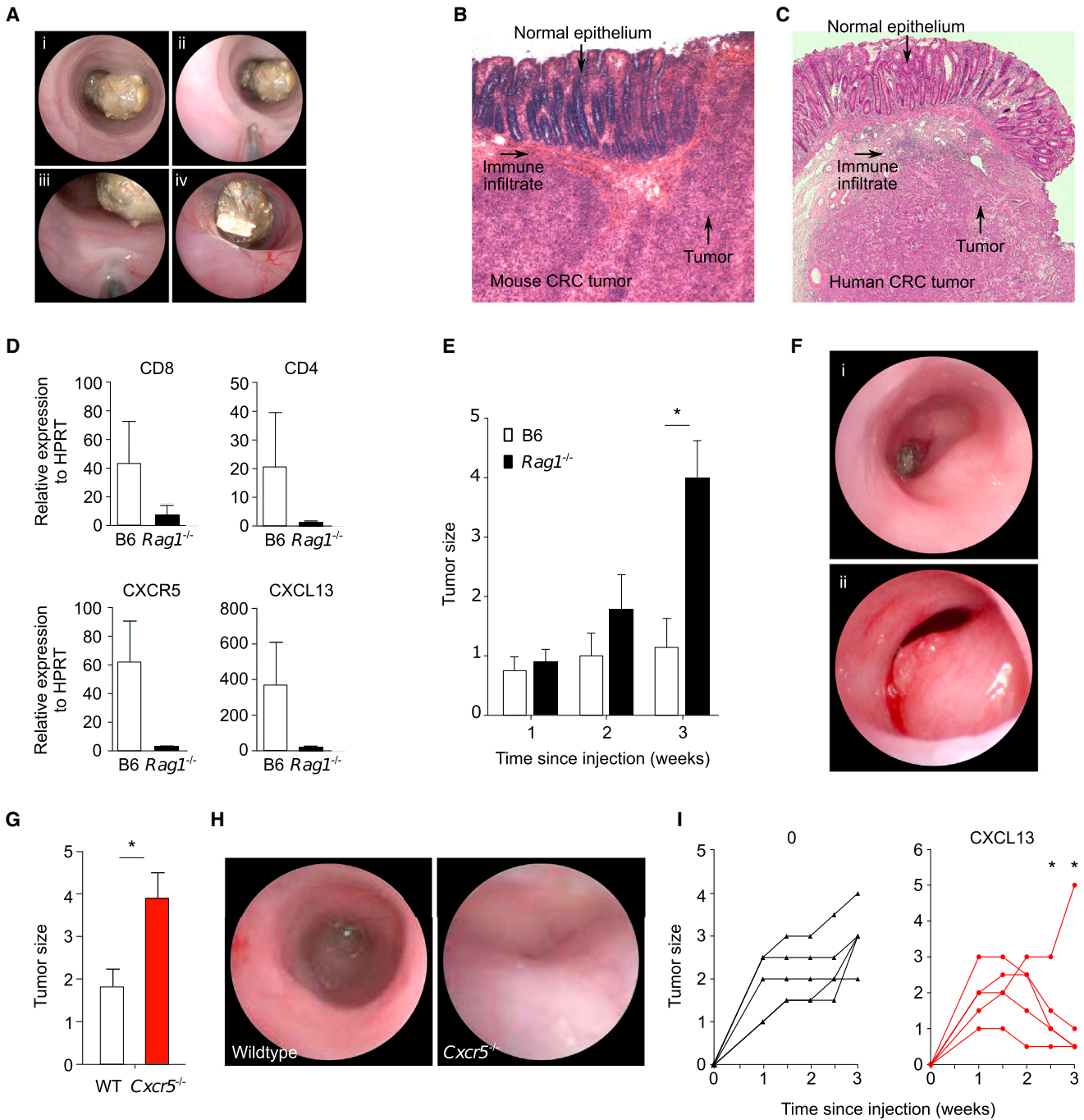


**Figure 7. Immunosurveillance and CXCL13-CXCR5 Signaling in a Murine Orthotopic CRC Model**

(A) The murine CRC cell line MC38 ( $10^4$ ) was injected endoscopically into the submucosa of syngenic C57Bl/6 and *Rag1*<sup>-/-</sup> mice (i-iv). Tumor growth was monitored by endoscopy every week.

(B and C) H&E staining of murine MC38 (A) and human (B) CRC tissue sections. Representative images for murine and human CRC tissue sections are shown. Immune = area showing an immune cell infiltration at the tumor margin. Tum = tumor center.

(D) Normalized gene expression of various markers of the adaptive immune response.  $n = 3$  per group. Data are presented as means  $\pm$  SEM.

(E) Endoscopic scoring of tumor growth after the endoscopic injection of MC38 cells ( $10^4$ ) into the submucosa of C57Bl/6 and *Rag1*<sup>-/-</sup> mice. Endoscopy was performed at the indicated time points. The experiment was repeated twice.  $n = 5$  per group. Data are presented as means  $\pm$  SEM.

(F) Tumor growth in C57Bl/6 mice (i) and *Rag1*<sup>-/-</sup> mice (ii) was monitored by endoscopy at 3 weeks.

(G and H) Endoscopic scoring of tumor growth after 3 weeks of endoscopic injection of MC38 cells ( $10^4$ ) into the submucosa of C57Bl/6 and *Cxcr5*<sup>-/-</sup> mice. Data are presented as means  $\pm$  SEM.

(I) Endoscopic scoring of tumor growth after the endoscopic injection of MC38 cells ( $10^5$ ) with or without injection of recombinant CXCL13 into the submucosa of wild-type mice.

of these tumors is comparable to human colorectal cancer in that the tumors show infiltrative growth through the mucosa and an immune response both within the tumor and at the tumor margin (Figures 7B and 7C).

For a functional analysis of the adaptive immune system during CRC progression, we exposed *Rag1*<sup>-/-</sup> and wild-type mice to the endoscopic orthotopic tumor model. As expected, tumors of wild-type mice expressed various markers (CD8, CD4, CXCR5, and CXCL13) of the adaptive immune response; these markers were expressed to a markedly lower level in *Rag1*<sup>-/-</sup> mice (Figure 7D). The markers included the chemokine CXCL13 and its receptor CXCR5, suggesting a contribution of CXCL13 signaling and Tfh-B cell interactions to the adaptive anti-tumor immune response. Importantly, the growth of orthotopic MC38 tumors was significantly accelerated in *Rag1*<sup>-/-</sup> mice in comparison to wild-type mice and therefore indicated a functionally relevant immune control in a CRC mouse tumor model (Figures 7E and 7F). To validate these findings, we used two additional mouse models. *Cxcr5*<sup>-/-</sup> mice were subjected to endoscopic orthotopic injection of tumor cells. These mice presented with an accelerated tumor growth compared to growth in wild-type mice (Figures 7G and 7H). Finally, we injected recombinant CXCL13 endoscopically within the colonic submucosa of wild-type mice. Whereas all control mice (5/5) experienced tumor growth, 80% (4/5) of CXCL13-treated mice experienced tumor rejection (Fisher exact-test  $p < 0.05$  at weeks 2.5 and 3 after injection) (Figure 7I). Thus, the good prognostic values of cytotoxic T cells, CXCL13, Tfh, and B cells were confirmed in murine orthotopic CRC models showing decreased tumor burden.

## DISCUSSION

Uncovering the complex interactions of tumors with their microenvironment is of major importance in understanding defense against cancer (Galon et al., 2013). After characterizing the majority of the immune subsets infiltrating colorectal tumors, we placed the immune-tumor interface into a spatiotemporal context. This led to a new perspective of host defense, the immune landscape within the tumor, and revealed a central role of Tfh and B cells.

Herein, we answered four questions. First, which immune cell subpopulations present within the tumor, evolved over time, and are associated with tumor progression from stages T1 to T4? Second, among all immune cells, which are the important ones for tumor recurrence and patient survival? Third, can we understand the spatiotemporal dynamics of the immune reaction in order to open new therapeutic perspectives at different stages of the disease? Fourth, which mechanisms are associated with different densities of intratumor immune cells?

This comprehensive analysis of the most innate and adaptive immune cells infiltrating tumors provides the most complete picture of the immune reaction in human cancer so far. Highly expressed markers of purified immune cell subsets comprised a compendium; a resource useful for scientists wishing to analyze immune cells. Using the immunome, we investigated the complexity of the immune signature in colorectal cancer tumors. The caveat, however, is that the correlations we observed could be due to the contribution of multiple factors. The correlation

among genes could reflect variation in cell frequencies. Contrary to this, within the tumor microenvironment, specific immunome genes could also be expressed in other cell types. Gene expression might be prone to bias when applied to extremely heterogeneous and dynamic systems, where the gene expression profile of pure samples cannot be considered an accurate parameter for normalization. This is the case for tumor specimens, where the gene-expression profiles in predefined cell subsets can dramatically change under the influence of cytokines, chemokines, and additional neighboring cells within the tumor microenvironment. However, here the purified immune cells were investigated in different activation states, and only the most representative genes (those overexpressed regardless of the activation status) were kept. Furthermore, in the immunome compendium, genes were selected on the basis of being highly expressed on a specific cell type, and those encoding known specific immune cell markers (CD19, CD209, LAMP3, CD3E, IFNG, and PRF1) were found; thus, there existed a robust validation of the selection criteria. Because of the limitations of gene expression profiles, additional approaches, such as flow-cytometry and immunohistochemistry, are recommended to validate a deep characterization of the cellular components of a tumor biopsy. In the current study, multiple techniques and experimental approaches (DNA microarray [Affymetrix], qPCR, FACS, IHC, and mouse models) were used. Importantly, concordant results were found with all approaches, reinforcing our results and conclusions.

We found that the immune infiltrates vary considerably from tumor to tumor and that they evolve over time. In addition, we present here the immune landscape in colorectal tumors and its evolution with tumor progression. Variable densities (“mountains” and “hills”) of immune cell subsets from the innate and adaptive compartments are shown. Adaptive immune cells functionally associate into a core network reflecting tumor regions. The tight association of B and T cells could reflect how B cells modulate T cell responses by presenting antigens, providing costimulation, and secreting cytokines (Lund and Randall, 2010). Densities of Tfh cells and most innate cells rose only in early-stage tumors, whereas most T cell densities decreased along with tumor progression. Importantly, B cells, which are part of the core immune cell network and are associated with prolonged survival, increased at a late stage and had a dual effect on recurrence and tumor progression. Distinct B cell subpopulations found at the tumor microenvironment could play different roles, protumoral or antitumoral (DeNardo et al., 2010; Lund and Randall, 2010; Pape et al., 2011). In human colorectal tumors, B cells were strongly correlated with Tfh cells and were associated with a good prognosis. It is evident that virtually all of the T cells in the network exert a marked positive effect on clinical outcome, as do B cells. In this regard it was of interest that the Tfh cells also exerted a positive effect. In contrast, macrophages, although part of the network and present at high density, did not significantly affect tumor recurrence. A strong and effective protection against relapse does not necessarily depend on the density of the immune cells. Thus, immune cell types, even at low density, have major importance for tumor recurrence.

As recently reviewed (Tangye et al., 2013), Tfh cells mediate B cell responses and might underlie immunological diseases

such as autoimmunity, immunodeficiency, and lymphoma. Here, we investigated Tfh cells in solid tumors. The generation of Tfh cells is mediated by IL-21 independently of other T helper subsets (Nurieva et al., 2008). Through the IL-21 pathway, Tfh cells can give rise to transferrable memory cells with plasticity; such cells differentiated after recall into conventional effector helper T cells and Tfh cells. It was demonstrated that Tfh cells were not terminally differentiated but instead retained the flexibility to be recruited into other helper T cell subsets and nonlymphoid tissues (Lüthje et al., 2012). Interestingly, it was shown that early Th1 cell differentiation is marked by a Tfh-cell-like transition (Nakayamada et al., 2011). Furthermore, in a transgenic mouse model, IL-21 promotes CD8<sup>+</sup> CTL activity via the transcription factor T-bet (Sutherland et al., 2013). Here we show major correlations between CXCL13, IL-21, Th1, and Tfh cells, supporting the central role of these factors in shaping the immune contexture in human tumors.

Tfh cells provide help to B cells for the generation of germinal centers and long-term protective humoral responses. Persistent antigen and germinal center B cells sustain T<sub>FH</sub> cell responses and phenotype (Baumjohann et al., 2013). It is also recognized that Tfh cells, display substantial flexibility and plasticity and participate in shaping the T cell response (Cannon et al., 2013). CXCL13 is a hallmark of Tfh cells, and CXCR5 has been identified as the receptor for CXCL13. It was also reported that CXCL13 is an agonist for the human CXCR3 receptor (Jenh et al., 2001). Thus, CXCL13 produced within the tumor and by Tfh cells in proximity to the tertiary lymphoid structure might also be a chemotactic agent for activated and memory T cells (Jenh et al., 2001; Mlecnik et al., 2010b). Furthermore, IL-21 transgenic mice revealed that overexpression of IL-21 directly promoted massive CD8<sup>+</sup> memory T cell accumulation (Allard et al., 2007). Indeed, we found a strong and significant correlation between CXCL13, IL-21, and these adaptive immune cells within the tumor-infiltrating immune cell network.

Thus, we revealed herein major immune components from the immune context associated with prolonged survival and the absence of tumor recurrence (Angell and Galon, 2013; Fridman et al., 2012; Galon et al., 2007). Through the production of CXCL13, Tfh cells activate a positive loop associated with increased intratumor densities of B, Tfh, Th1, cytotoxic, and memory T cells in human colorectal tumors. Therefore, in addition to memory T cells (Galon et al., 2006), CXCL13 and IL-21 constitute, along with B cells and Tfh cells, the main antitumor players. These adaptive immune cells are likely to ensure long-term survival of the patients because they can acquire a memory phenotype.

The results reported here add to those published previously (Galon et al., 2006; Pagès et al., 2005) in several important ways. By investigating most of the infiltrating immune cells, we have been able to show a complete view of the immune compartment of the tumor microenvironment. Among all the immune cell subpopulations, B cells, T cells, and Tfh cells have a major role in human colorectal cancer. Furthermore, we developed unique endoscopic orthotopic CRC mouse models to demonstrate the role of the adaptive anti-tumor immune response. The growth of mouse colon tumor cells was signifi-

cantly accelerated in *Rag1*<sup>-/-</sup> and in *Cxcr5*<sup>-/-</sup> mice in comparison to wild-type mice, whereas tumors were rejected upon injection of CXCL13. This demonstrates the functional relevant immune control in a CRC mouse model.

Spatiotemporal associations between immune populations with a strong impact on patient survival were revealed. We present sophisticated and synthetic methods of visualizing the coordination and the strength of the host intratumoral immune reaction along with tumor progression. Furthermore, integrating the data into a network model representing the entire tumor allowed us to interrogate dynamic networks in the three-dimensional immune landscape along with tumor progression over time and with tumor recurrence. The investigation of amplifications or deletions of all chemokines and chemokine receptors within colorectal tumors revealed the major role of CXCL13 with regard to tumor recurrence and patient survival. Finally, our data support a mechanism resulting in high or low densities of intratumor Tfh and B cells within the IM of CRC tumors with major clinical relevance.

The integrated analysis of diverse data sets might circumvent challenges related to the staggering complexity of multifactorial diseases such as cancer (Bindea et al., 2010). Researchers have started to apply systems biology approaches to the study of the immune system (Benoist et al., 2006; Gilchrist et al., 2006; Tegnér et al., 2006) and to modeling the immune response (Kim et al., 2009). Emerging bioinformatics resources are now aiding these types of analyses (Bindea et al., 2013; Bindea et al., 2009; Shannon et al., 2003). At this point, we are reaching a level where we may be able to capture the spatiotemporal dynamics of complex disease processes. Our data highlight the power of integrative cancer-immunology approaches to help researchers understand the challenging issues of tumor progression and tumor recurrence (Galon et al., 2013). The landscape representation greatly improved the visualization and the interpretation of the coordination of the intratumoral immune cell densities.

The information presented here might be of major clinical importance. The different patterns of evolution of specific immune cell subpopulations along with tumor progression could lead to different strategies for the treatment of patients with colorectal cancer. This knowledge can help scientists to prioritize research, better understand disease pathogenesis, and gain clues into how we might therapeutically manipulate this system.

## EXPERIMENTAL PROCEDURES

### Colorectal Cancer Patients

Colorectal cancer patients who underwent a primary resection of their tumor at the Laennec-HEGP Hospitals between 1996 and 2004 were reviewed and previously described. Histopathological and clinical findings were scored according to the Union for International Cancer Control TNM staging system (Table S7). Ethical, legal and social implications were reviewed by an ethics review board. All experiments were performed according to the Helsinki guidelines.

### Mouse Model

Endoscopic injection of murine MC38 colon tumor cells in the submucosa of the colon of C57Bl/6, *Rag1*<sup>-/-</sup>, and *Cxcr5*<sup>-/-</sup> mice. The needle was positioned inside the working channel of the endoscope so that there would be no damage to the colonic mucosa. After insertion of the endoscope, the tip of

the needle was carefully inserted through the mucosa into the submucosa, and a low number of cells ( $10^4$ – $10^5$ ) were injected into the submucosa. Recombinant CXCL13 was injected similarly. During subsequent weeks, tumor growth was analyzed via colon endoscopy.

### Experiments

DNA microarray experiments were performed with Affymetrix U133A Plus arrays. Quantitative real-time TaqMan PCR was performed with low-density arrays and the 7900 robotic real-time PCR system (Applied Biosystems). Immunohistochemistry on tissue microarray sections was performed as previously described (Galon et al., 2006). Migration assays on fresh infiltrating cells are described in detail in the [Supplemental Information](#). aCGH was carried out on a whole-genome oligonucleotide microarray platform (44B, Agilent Technologies).

### Datasets

The data sets used in this study are publicly available (ArrayExpress [Ancona et al., 2006; Parkinson et al., 2007; Wendt et al., 2006], Gene Expression Omnibus [Barrett et al., 2005; Hycza et al., 2007; Provenzani et al., 2006], and Garvan Institute dataset [Chtanova et al., 2005]) and were all generated with the HG-U133A Affymetrix platform. [Supplemental Experimental Procedures](#) and any associated references are available in the online version of the paper.

### Statistical Analysis

Correlation matrices were created with Pearson correlation. All bar plots are shown as mean  $\pm$  standard error of the mean (SEM). The normality of the data was tested with the Shapiro-Wilk test. For pairwise comparisons of parametric and nonparametric data, the Student's t test and Mann-Whitney-Wilcoxon rank-sum test, respectively, were used. The hazard ratio (Cox proportional hazards model) and the log-rank test were used for comparing disease-free and overall survival between patients in different groups. To avoid over-fitting, we corrected hazard ratios and log-rank p values obtained by the "minimum p value" approach by using the methods suggested by Hollander et al. (Holländer et al., 2004) and Altman et al. (Altman et al., 1994), respectively. The predictive performance of each individual marker was assessed by the Harrell's concordance index (c index) (Harrell et al., 1996) and time-dependent c index ( $C_T$  index) derived from time-dependent ROC analysis (Heagerty and Zheng, 2005). Throughout the text, a p value  $< 0.05$  is considered statistically significant. All analyses were performed with the statistical software R (survival package and risksetROC packages) implemented as a statistical module in TME.db (Mlecnik et al., 2010a). Functional and correlation analyses were performed with CluePedia and ClueGO (Bindea et al., 2013; Bindea et al., 2009) within the Cytoscape framework (Shannon et al., 2003).

### SUPPLEMENTAL INFORMATION

Supplemental Information includes Supplemental Experimental Procedures, a list of CEL files included in the immunome analysis, six figures, seven tables, and one movie and can be found with this article online at <http://dx.doi.org/10.1016/j.immuni.2013.10.003>.

### ACKNOWLEDGMENTS

We are grateful to Ion Gresser for providing helpful comments and critical review of the manuscript. This work was supported by grants from the National Cancer Institute of France (INCa), the Canceropole Ile de France, Ville de Paris, MedImmune, INSERM, the Austrian Federal Ministry of Science and Research (GEN-AU project Bioinformatics Integration Network), Qatar National Research Fund under its National Priorities Research Program award number NPRP09-1174-3-291, the European Commission (7FP, Geninca Consortium, grant 202230), and the LabEx Immuno-oncology.

Received: January 23, 2013

Accepted: July 25, 2013

Published: October 17, 2013

### REFERENCES

- Allard, E.L., Hardy, M.P., Leignadier, J., Marquis, M., Rooney, J., Lehoux, D., and Labrecque, N. (2007). Overexpression of IL-21 promotes massive CD8+ memory T cell accumulation. *Eur. J. Immunol.* 37, 3069–3077.
- Altman, D.G., Lausen, B., Sauerbrei, W., and Schumacher, M. (1994). Dangers of using "optimal" cutpoints in the evaluation of prognostic factors. *J. Natl. Cancer Inst.* 86, 829–835.
- Ancona, N., Maglietta, R., Piepoli, A., D'Addabbo, A., Cotugno, R., Savino, M., Liuni, S., Carella, M., Pesole, G., and Perri, F. (2006). On the statistical assessment of classifiers using DNA microarray data. *BMC Bioinformatics* 7, 387.
- Angell, H., and Galon, J. (2013). From the immune contexture to the Immunoscore: The role of prognostic and predictive immune markers in cancer. *Curr. Opin. Immunol.* 25, 261–267.
- Atreya, I., and Neurath, M.F. (2008). Immune cells in colorectal cancer: Prognostic relevance and therapeutic strategies. *Expert Rev. Anticancer Ther.* 8, 561–572.
- Barrett, T., Suzek, T.O., Troup, D.B., Wilhite, S.E., Ngau, W.C., Ledoux, P., Rudnev, D., Lash, A.E., Fujibuchi, W., and Edgar, R. (2005). NCBI GEO: mining millions of expression profiles—Database and tools. *Nucleic Acids Res.* 33(Database issue), D562–D566.
- Baumjohann, D., Preite, S., Reboldi, A., Ronchi, F., Ansel, K.M., Lanzavecchia, A., and Sallusto, F. (2013). Persistent antigen and germinal center B cells sustain T follicular helper cell responses and phenotype. *Immunity* 38, 596–605.
- Benoist, C., Germain, R.N., and Mathis, D. (2006). A plaidoyer for 'systems immunology'. *Immunol. Rev.* 210, 229–234.
- Bindea, G., Mlecnik, B., Hackl, H., Charoentong, P., Tosolini, M., Kirilovsky, A., Fridman, W.H., Pagès, F., Trajanoski, Z., and Galon, J. (2009). ClueGO: a Cytoscape plug-in to decipher functionally grouped gene ontology and pathway annotation networks. *Bioinformatics* 25, 1091–1093.
- Bindea, G., Mlecnik, B., Fridman, W.H., Pagès, F., and Galon, J. (2010). Natural immunity to cancer in humans. *Curr. Opin. Immunol.* 22, 215–222.
- Bindea, G., Galon, J., and Mlecnik, B. (2013). CluePedia Cytoscape plugin: pathway insights using integrated experimental and in silico data. *Bioinformatics* 29, 661–663.
- Cannons, J.L., Lu, K.T., and Schwartzberg, P.L. (2013). T follicular helper cell diversity and plasticity. *Trends Immunol.* 34, 200–207.
- Chtanova, T., Newton, R., Liu, S.M., Weininger, L., Young, T.R., Silva, D.G., Bertoni, F., Rinaldi, A., Chappaz, S., Sallusto, F., et al. (2005). Identification of T cell-restricted genes, and signatures for different T cell responses, using a comprehensive collection of microarray datasets. *J. Immunol.* 175, 7837–7847.
- DeNardo, D.G., Andreu, P., and Coussens, L.M. (2010). Interactions between lymphocytes and myeloid cells regulate pro- versus anti-tumor immunity. *Cancer Metastasis Rev.* 29, 309–316.
- Deola, S., Panelli, M.C., Maric, D., Selleri, S., Dmitrieva, N.I., Voss, C.Y., Klein, H., Stroncek, D., Wang, E., and Marincola, F.M. (2008). Helper B cells promote cytotoxic T cell survival and proliferation independently of antigen presentation through CD27/CD70 interactions. *J. Immunol.* 180, 1362–1372.
- Finn, O.J. (2008). *Cancer immunology*. *N. Engl. J. Med.* 358, 2704–2715.
- Fridman, W.H., Pagès, F., Sautès-Fridman, C., and Galon, J. (2012). The immune contexture in human tumours: impact on clinical outcome. *Nat. Rev. Cancer* 12, 298–306.
- Galon, J., Costes, A., Sanchez-Cabo, F., Kirilovsky, A., Mlecnik, B., Lagorce-Pagès, C., Tosolini, M., Camus, M., Berger, A., Wind, P., et al. (2006). Type, density, and location of immune cells within human colorectal tumors predict clinical outcome. *Science* 313, 1960–1964.
- Galon, J., Fridman, W.H., and Pagès, F. (2007). The adaptive immunologic microenvironment in colorectal cancer: a novel perspective. *Cancer Res.* 67, 1883–1886.
- Galon, J., Angell, H.K., Bedognetti, D., and Marincola, F.M. (2013). The continuum of cancer immunosurveillance: Prognostic, predictive, and mechanistic signatures. *Immunity* 39, 11–26.

- Gilchrist, M., Thorsson, V., Li, B., Rust, A.G., Korb, M., Roach, J.C., Kennedy, K., Hai, T., Bolouri, H., and Aderem, A. (2006). Systems biology approaches identify ATF3 as a negative regulator of Toll-like receptor 4. *Nature* *441*, 173–178.
- Harrell, F.E., Jr., Lee, K.L., and Mark, D.B. (1996). Multivariable prognostic models: Issues in developing models, evaluating assumptions and adequacy, and measuring and reducing errors. *Stat. Med.* *15*, 361–387.
- Heagerty, P.J., and Zheng, Y. (2005). Survival model predictive accuracy and ROC curves. *Biometrics* *61*, 92–105.
- Holländer, N., Sauerbrei, W., and Schumacher, M. (2004). Confidence intervals for the effect of a prognostic factor after selection of an 'optimal' cutpoint. *Stat. Med.* *23*, 1701–1713.
- Hyrcoza, M.D., Kovacs, C., Loutfy, M., Halpenny, R., Heisler, L., Yang, S., Wilkins, O., Ostrowski, M., and Der, S.D. (2007). Distinct transcriptional profiles in ex vivo CD4+ and CD8+ T cells are established early in human immunodeficiency virus type 1 infection and are characterized by a chronic interferon response as well as extensive transcriptional changes in CD8+ T cells. *J. Virol.* *81*, 3477–3486.
- Jemal, A., Siegel, R., Ward, E., Murray, T., Xu, J., Smigal, C., and Thun, M.J. (2006). Cancer statistics, 2006. *CA Cancer J. Clin.* *56*, 106–130.
- Jenh, C.H., Cox, M.A., Hipkin, W., Lu, T., Pugliese-Sivo, C., Gonsiorek, W., Chou, C.C., Narula, S.K., and Zavodny, P.J. (2001). Human B cell-attracting chemokine 1 (BCA-1; CXCL13) is an agonist for the human CXCR3 receptor. *Cytokine* *15*, 113–121.
- June, C.H. (2007a). Adoptive T cell therapy for cancer in the clinic. *J. Clin. Invest.* *117*, 1466–1476.
- June, C.H. (2007b). Principles of adoptive T cell cancer therapy. *J. Clin. Invest.* *117*, 1204–1212.
- Kim, P.S., Levy, D., and Lee, P.P. (2009). Modeling and simulation of the immune system as a self-regulating network. *Methods Enzymol.* *467*, 79–109.
- King, C., Tangye, S.G., and Mackay, C.R. (2008). T follicular helper (TFH) cells in normal and dysregulated immune responses. *Annu. Rev. Immunol.* *26*, 741–766.
- Koebel, C.M., Vermi, W., Swann, J.B., Zerafa, N., Rodig, S.J., Old, L.J., Smyth, M.J., and Schreiber, R.D. (2007). Adaptive immunity maintains occult cancer in an equilibrium state. *Nature* *450*, 903–907.
- Lund, F.E., and Randall, T.D. (2010). Effector and regulatory B cells: Modulators of CD4+ T cell immunity. *Nat. Rev. Immunol.* *10*, 236–247.
- Lüthje, K., Kallies, A., Shimohakamada, Y., Belz, G.T., Light, A., Tarlinton, D.M., and Nutt, S.L. (2012). The development and fate of follicular helper T cells defined by an IL-21 reporter mouse. *Nat. Immunol.* *13*, 491–498.
- Mlecnik, B., Sanchez-Cabo, F., Charoentong, P., Bindea, G., Pagès, F., Berger, A., Galon, J., and Trajanoski, Z. (2010a). Data integration and exploration for the identification of molecular mechanisms in tumor-immune cells interaction. *BMC Genomics* *11*(Suppl 1), S7.
- Mlecnik, B., Tosolini, M., Charoentong, P., Kirilovsky, A., Bindea, G., Berger, A., Camus, M., Gillard, M., Bruneval, P., Fridman, W.H., et al. (2010b). Biomolecular network reconstruction identifies T-cell homing factors associated with survival in colorectal cancer. *Gastroenterology* *138*, 1429–1440.
- Mlecnik, B., Tosolini, M., Kirilovsky, A., Berger, A., Bindea, G., Meatchi, T., Bruneval, P., Trajanoski, Z., Fridman, W.H., Pagès, F., and Galon, J. (2011). Histopathologic-based prognostic factors of colorectal cancers are associated with the state of the local immune reaction. *J. Clin. Oncol.* *29*, 610–618.
- Nakayamada, S., Kanno, Y., Takahashi, H., Jankovic, D., Lu, K.T., Johnson, T.A., Sun, H.W., Vahedi, G., Hakim, O., Handon, R., et al. (2011). Early Th1 cell differentiation is marked by a Tfh cell-like transition. *Immunity* *35*, 919–931.
- Nurieva, R.I., Chung, Y., Hwang, D., Yang, X.O., Kang, H.S., Ma, L., Wang, Y.H., Watowich, S.S., Jetten, A.M., Tian, Q., and Dong, C. (2008). Generation of T follicular helper cells is mediated by interleukin-21 but independent of T helper 1, 2, or 17 cell lineages. *Immunity* *29*, 138–149.
- Pagès, F., Berger, A., Camus, M., Sanchez-Cabo, F., Costes, A., Molitor, R., Mlecnik, B., Kirilovsky, A., Nilsson, M., Damotte, D., et al. (2005). Effector memory T cells, early metastasis, and survival in colorectal cancer. *N. Engl. J. Med.* *353*, 2654–2666.
- Pagès, F., Kirilovsky, A., Mlecnik, B., Asslaber, M., Tosolini, M., Bindea, G., Lagorce, C., Wind, P., Marliot, F., Bruneval, P., et al. (2009). In situ cytotoxic and memory T cells predict outcome in patients with early-stage colorectal cancer. *J. Clin. Oncol.* *27*, 5944–5951.
- Pape, K.A., Taylor, J.J., Maul, R.W., Gearhart, P.J., and Jenkins, M.K. (2011). Different B cell populations mediate early and late memory during an endogenous immune response. *Science* *331*, 1203–1207.
- Parkinson, H., Kapushesky, M., Shojatalab, M., Abeygunawardena, N., Coulson, R., Farne, A., Holloway, E., Kolesnykov, N., Lilja, P., Lukk, M., et al. (2007). ArrayExpress—A public database of microarray experiments and gene expression profiles. *Nucleic Acids Res.* *35* (Database issue), D747–D750.
- Provenzani, A., Fronza, R., Loreni, F., Pascale, A., Amadio, M., and Quattrone, A. (2006). Global alterations in mRNA polysomal recruitment in a cell model of colorectal cancer progression to metastasis. *Carcinogenesis* *27*, 1323–1333.
- Schreiber, R.D., Old, L.J., and Smyth, M.J. (2011). Cancer immunoediting: Integrating immunity's roles in cancer suppression and promotion. *Science* *331*, 1565–1570.
- Shankaran, V., Ikeda, H., Bruce, A.T., White, J.M., Swanson, P.E., Old, L.J., and Schreiber, R.D. (2001). IFN $\gamma$  and lymphocytes prevent primary tumour development and shape tumour immunogenicity. *Nature* *410*, 1107–1111.
- Shannon, P., Markiel, A., Ozier, O., Baliga, N.S., Wang, J.T., Ramage, D., Amin, N., Schwikowski, B., and Ideker, T. (2003). Cytoscape: a software environment for integrated models of biomolecular interaction networks. *Genome Res.* *13*, 2498–2504.
- Smyth, M.J., Dunn, G.P., and Schreiber, R.D. (2006). Cancer immunosurveillance and immunoediting: the roles of immunity in suppressing tumor development and shaping tumor immunogenicity. *Adv. Immunol.* *90*, 1–50.
- Sturn, A., Quackenbush, J., and Trajanoski, Z. (2002). Genesis: cluster analysis of microarray data. *Bioinformatics* *18*, 207–208.
- Sutherland, A.P., Joller, N., Michaud, M., Liu, S.M., Kuchroo, V.K., and Grusby, M.J. (2013). IL-21 promotes CD8+ CTL activity via the transcription factor T-bet. *J. Immunol.* *190*, 3977–3984.
- Tangye, S.G., Ma, C.S., Brink, R., and Deenick, E.K. (2013). The good, the bad and the ugly - TFH cells in human health and disease. *Nat. Rev. Immunol.* *13*, 412–426.
- Tegnér, J., Nilsson, R., Bajic, V.B., Björkegren, J., and Ravasi, T. (2006). Systems biology of innate immunity. *Cell. Immunol.* *244*, 105–109.
- Tsafir, D., Baccolod, M., Selvanayagam, Z., Tsafir, I., Shia, J., Zeng, Z., Liu, H., Krier, C., Stengel, R.F., Barany, F., et al. (2006). Relationship of gene expression and chromosomal abnormalities in colorectal cancer. *Cancer Res.* *66*, 2129–2137.
- Wang, E., Panelli, M.C., Monsurro, V., and Marincola, F.M. (2004). A global approach to tumor immunology. *Cell. Mol. Immunol.* *1*, 256–265.
- Wang, E., Worschech, A., and Marincola, F.M. (2008). The immunologic constant of rejection. *Trends Immunol.* *29*, 256–262.
- Weitz, J., Koch, M., Debus, J., Höhler, T., Galle, P.R., and Büchler, M.W. (2005). Colorectal cancer. *Lancet* *365*, 153–165.
- Wendt, K., Wilk, E., Buyny, S., Buer, J., Schmidt, R.E., and Jacobs, R. (2006). Gene and protein characteristics reflect functional diversity of CD56dim and CD56bright NK cells. *J. Leukoc. Biol.* *80*, 1529–1541.